



Universiteit
Leiden
The Netherlands

Development of a kidney-on-a-chip model for compound screening and transport studies

Vormann, M.K.

Citation

Vormann, M. K. (2021, September 9). *Development of a kidney-on-a-chip model for compound screening and transport studies*. Retrieved from <https://hdl.handle.net/1887/3209238>

Version: Publisher's Version

License: [Licence agreement concerning inclusion of doctoral thesis in the Institutional Repository of the University of Leiden](#)

Downloaded from: <https://hdl.handle.net/1887/3209238>

Note: To cite this publication please use the final published version (if applicable).

Cover Page



Universiteit Leiden



The handle <https://hdl.handle.net/1887/3209238> holds various files of this Leiden University dissertation.

Author: Vormann, M.K.

Title: Development of a kidney-on-a-chip model for compound screening and transport studies

Issue Date: 2021-09-09



Chapter 5

Modelling and Prevention of Acute Kidney Injury Through Ischemia and Reperfusion in a Combined Human Renal Proximal Tubule/Blood Vessel-on-a-Chip.

MK Vormann, LM Tool, M Ohbuchi, L Gijzen, R van Vught, T Hankemeier, F Kiyonaga, T Kawabe, T Goto, A Fujimori, P Vulto, HL Lanz & K Tetsuka

Based on:

Kidney360 - Submitted (2021)

Significance Statement

Renal ischemia/reperfusion injury (rIRI) is one of the major causes associated with tubular damage leading to acute kidney injury (AKI). In this study we modelled rIRI-induced AKI *in vitro* in a reconstituted human renal proximal tubule-on-a-chip with endothelial vessels through the control of ischemic parameters (i.e. oxygen, nutrients, and flow). The ischemic conditions had a detrimental effect on the proximal tubule, that was significantly amplified by subsequent reperfusion. Adenosine was shown to protect from disruption of epithelial cells and caspase 3/7 activation. As the platform is amenable to screening, this model will support pathophysiological research as well as drug discovery.

Abstract

Background Renal ischemia/reperfusion injury (rIRI) is one of the major causes of acute kidney injury (AKI). While animal models are suitable for investigating systemic symptoms of AKI they are limited in translatability. Human *in vitro* models are crucial in giving mechanistic insights into rIRI, however, they miss out on crucial aspects as reperfusion injury and the multi tissue aspect of AKI.

Methods We advanced the current renal proximal tubule-on-a-chip model to a coculture model with a perfused endothelial vessel separated by an extracellular matrix (ECM). The coculture was characterized for its three-dimensional structure, protein expression, and response to nephrotoxins. Then, rIRI was captured through control of oxygen levels, nutrient availability, and perfusion flow settings. Injury was quantified through morphological assessment, caspase 3/7 activation, and cell viability.

Results The combination of low oxygen, reduced glucose, and interrupted flow was potent to disturb the proximal tubules. This effect was strongly amplified upon reperfusion. Endothelial vessels were less sensitive to the ischemia-reperfusion parameters. Adenosine treatment showed a protective effect on the disruption of the epithelium and on the caspase 3/7 activation.

Conclusions A human *in vitro* rIRI model was developed using a coculture of a proximal tubule and blood vessel on-a-chip, which was used to characterize the renoprotective effect of adenosine. The robustness of the model and assays in combination with the throughput of the platform make it ideal to advance pathophysiological research and enable the development of novel therapeutic modalities.

Introduction

Acute kidney injury (AKI) is a severe medical problem with a high mortality rate. Every year around 1.7 million people die of AKI worldwide [1], [2]. Since the kidney is responsible for eliminating waste products from the blood it encounters high concentrations of xenobiotics and is therefore

vulnerable for (drug-induced) toxicity [3], [4]. In the kidney, renal proximal tubule epithelial cells (RPTEC) express many ATP-dependent transporters and play important roles in re-absorption of essential nutrients. RPTEC have a high energy demand to drive active transporters, and renal blood flow supplies the required oxygen [5], [6]. Patients with a disrupted renal flow, either because of pre-renal hypoperfusion (e.g. heart failure, hemorrhage) or post-renal obstruction (e.g. cancer, blood clot) also suffer from AKI [3], [7]. Renal ischemia/reperfusion injury (rIRI) causes a loss of function and cell damage of the proximal tubule structure, ultimately leading to AKI [8]–[10]. Recently, AKI has been extensively researched as a symptom following SARS-CoV-2 infection [11].

For investigating the pathophysiology of rIRI and drug screening for AKI, animal models are widely used to capture systemic symptoms of AKI [12]. However, here a significant species difference between animal and human is observed [13]. Not all drug candidates that showed efficacy in animal models showed efficacy in AKI treatment in clinical trials. *In vitro* cellular models are also applied for elucidation of rIRI/AKI mechanistic insights [14]. Unfortunately, traditional 2D culture settings of RPTEC lack their typical structure and their associated functionality [15], [16]. *In vitro* experiments do allow for a controlled environment, allowing manipulation of specific variables, and enabling higher reproducibility [14]. Finally, replacement of animal models is expected to reduce costs and time, as well as increase the throughput and predictability [17], [18].

Human cellular models can be valuable tools for tackling rIRI and discovery of AKI preventive agents [19]. *In vitro* rIRI models have been reported that enable induction of hypoxia by chemical induction, enzymatic induction, or anaerobic chambers [14]. However, additional parameters are important to comprehensively mimic ischemia-inducing insults [20]. Loss of nutrients, loss of flow, and buildup of waste products, as well as the reset of all parameters upon reperfusion can cause damage and should be included in rIRI modelling. Recent advances in tissue engineering and microfluidic cell culture techniques have made significant progress in modelling key aspects of human organs *in vitro* [15]. For example, a 3D model of the proximal tubule comprising perfusion flow was established in a microfluidic chip setup [21]–[24]. Application of shear stress to the apical side is important as it regulates tight-junction and polarized transporter localization [25]–[28]. We have previously reported a human proximal tubule on-a-chip model comprised of 40 perfused proximal tubules grown against an extracellular matrix (ECM) [24]. We showed the utility of this model for assessing kidney toxicity, drug-drug interaction, and transporter function [24], [29], [30].

In this study, we developed an advanced model to study rIRI comprising a perfused 3D proximal tubule adjacent to a 3D perfused blood vessel. The proximal tubule and blood vessel are separated by a collagen 1 surrogate extracellular matrix (ECM). We characterized the culture using immunostaining for cell type specific markers and ensured correct polarization. We then validated the response to nephrotoxicants. We modelled rIRI by adjusting culture parameters

such as oxygen concentration, perfusion flow, and nutrients like glucose, followed by a return to normal culture conditions. Finally, we assessed the protective potential of adenosine, nicotinamide, and N-acetylcysteine (NAC) that have been reported to prevent rIRI in animal models [31]–[35]. We foresee that this new human rIRI model will provide a springboard for the development of preventative or curative treatments for ischemic AKI.

Materials and Methods

Cell culture

Human renal Proximal Tubule Epithelial Cells (RPTEC, Kidney PTEC Control Cells, SA7K Clone, Sigma-Aldrich, MTOX1030) were cultured on PureCol-coated (Advanced BioMetrix, 5005-B, diluted with 1:30 in HBSS (Sigma H6648), 20 min incubation at 37 °C) T75 flasks (Corning, 431464U) in MEME alpha Modification (Sigma, M4526) supplemented with RPTEC Complete Supplement (Sigma, MTOXRCSUP), L-glutamine (1.87 mM, Sigma, G7513), Gentamicin (28 µg/ml, Sigma, G1397) and Amphotericin B (14 ng/ml, Sigma, A2942). Cells were incubated in a humidified incubator (37 °C, 5 % CO₂) and medium was changed every 2-3 days. At 90-100 % confluency, cells were washed with HBSS, detached with accutase (Sigma, A6964), neutralized with culture medium, pelleted (140 g, 5 minutes), and used for seeding in the OrganoPlate. Cells were used up to passage 3.

Human umbilical vein endothelial cells (HUVEC, Lonza, C2519A) were cultured on surface treated T75 (Thermo Scientific, 156499) flasks in MV2 complete medium (Endothelial Cell Medium MV2, Promocell, C-22022) supplemented with Supplement Mix Endothelial Cell Growth Medium MV2 (Promocell, C-39226), and 1% Pen/Strep (Sigma, P4333). Cells were incubated in a humidified incubator (37 °C, 5 % CO₂) and medium was changed every 2-3 days. At 90-100 % confluency, cells were washed with HEPES-BSS (Lonza, CC-5022), detached with 0.025% Trypsin-EDTA (1X) solution (Lonza, CC-5012), neutralized with Trypsin Neutralizing Solution (Lonza, CC-5002), pelleted (200 g, 5 minutes), and used for seeding in the OrganoPlate. Cells were used up to passage 9.

Establishment of the RPTEC-HUVEC coculture

For all experiments, the OrganoPlate® 3-lane (Mimetas BV, 4003 400B) was used. Figure 1a shows a photograph of the bottom of the OrganoPlate, demonstrating the 40 microfluidic channel networks, glued to a standard 384-well plate. A zoom in on a single chip highlights the region of interest where three microfluidic channels join in the center (green circle, Fig. 1b). The 3 channels are separated by PhaseGuides, which are small ridges that prevent overflow between adjacent channels through meniscus pinning [36] (Fig. 1c, grey bars).

As a starting point for the seeding, we took the RPTEC monoculture protocol as previously described [24] and introduced a seeding procedure for an endothelial vessel alongside the RPTEC tubule (Fig. 1 d-f). In short, 2 µL of a liquefied ECM gel composed of 4 mg/ml collagen I was loaded

into the middle inlet of all 40 chips and let to polymerize (Fig. 1d step 1). The following day RPTECs were seeded against the gel to the top channel and allowed to adhere (Fig. 1d step 2). After attachment of the cells, medium was added and the OrganoPlate was placed in an incubator on an interval rocker platform (Mimetas BV, MI-OFPR-L) (+/- 7 degree angle, 8 minute interval) enabling a passive, bidirectional flow through the perfusion channels (Fig. 1d step 3).

HUVEC were added to the bottom channel of the microfluidic chip on day 2 (Fig. 1d step 4). HUVEC were detached as described above and re-suspended in MV2 complete medium at a concentration of 10×10^6 cells per ml. Medium from all bottom in- and outlets was aspirated, and the plate was turned 180° resulting in RPTEC tubes sitting in the bottom. 2 μ L of the HUVEC cell suspension was added to the (new) top left inlet. Subsequently, 1 μ L was aspirated via the outlet from the top channel to guide HUVEC through the system. The OrganoPlate was placed on its side at an angle of 75° to let the HUVEC attach to the ECM. After an incubation time of 60 minutes, medium from both channels was switched to coculture medium (50% CellBiologics complete human endothelial cell medium (basal medium with the growth factor supplement kit (H1168)) and 50% RPTEC complete medium). Perfusion was applied again resulting in fully grown tubules of RPTEC and HUVEC at day 6 (Fig. 1c, 1d step 5). Cocultures were used for experiments up to day 12. The timeline of coculture seeding was determined in an optimization study (data not shown) with RPTEC seeded on day 0, and HUVEC on day 2 (Fig. 1 d-f).

Immunohistochemistry

Cocultures were fixed by replacing the medium with 3.7% formaldehyde (Sigma, 252549) in HBSS (Sigma, 55037C) for 10 minutes. Tubules were washed with washing solution (4% fetal bovine serum (Gibco, 16140-071) in HBSS) and permeabilized (0.3% Triton X-100 (Sigma, T8787) in HBSS) for 10 minutes. Next, cultures were incubated for 45 minutes in blocking solution (2% FBS, 2% bovine serum albumin (BSA) (Sigma, A2153), and 0.1% Tween 20 (Sigma, P9416) in HBSS). Hereafter cultures were incubated with the primary antibodies, diluted in blocking solution, for 60 minutes at room temperature. Primary antibodies against Ms-a-ezrin (BD Biosciences, 610602, 1:200), Ms-a-acetylated tubulin (Sigma, T6793, 1:4000), Rb-a-Zonula occludens-1 (ZO-1) (Thermo Fischer, 61-7300, 1:125) and Rb-a-VE-cadherin (Abcam, Ab33168, 1:1000) were used. Subsequently, cultures were washed twice with washing solution for 5 minutes each and then incubated for 30 minutes at room temperature with secondary antibodies Gt-a-Ms IgG (H+L) Alexa Fluor 555 (Thermo Scientific, A21422, 1:250) and Gt-a-Rb IgG (H+L) Alexa Fluor 488 (Thermo Scientific, A32731, 1:250) diluted in blocking solution. After washing the tubules two times for 5 minutes, nuclei were stained with Hoechst 33342 (Thermo Fisher Scientific, H3570, 1:2000) in the last washing step. Fluorescent images for the 3D reconstructions were taken with the ImageXpress® Micro Confocal High-Content Imaging System (Molecular Devices). A z-stack of 220 μ m with 2 μ m between each image plane was acquired for DAPI, FITC, and TRITC channels. 3D reconstructions and maximum projections were created using ImageJ [37].

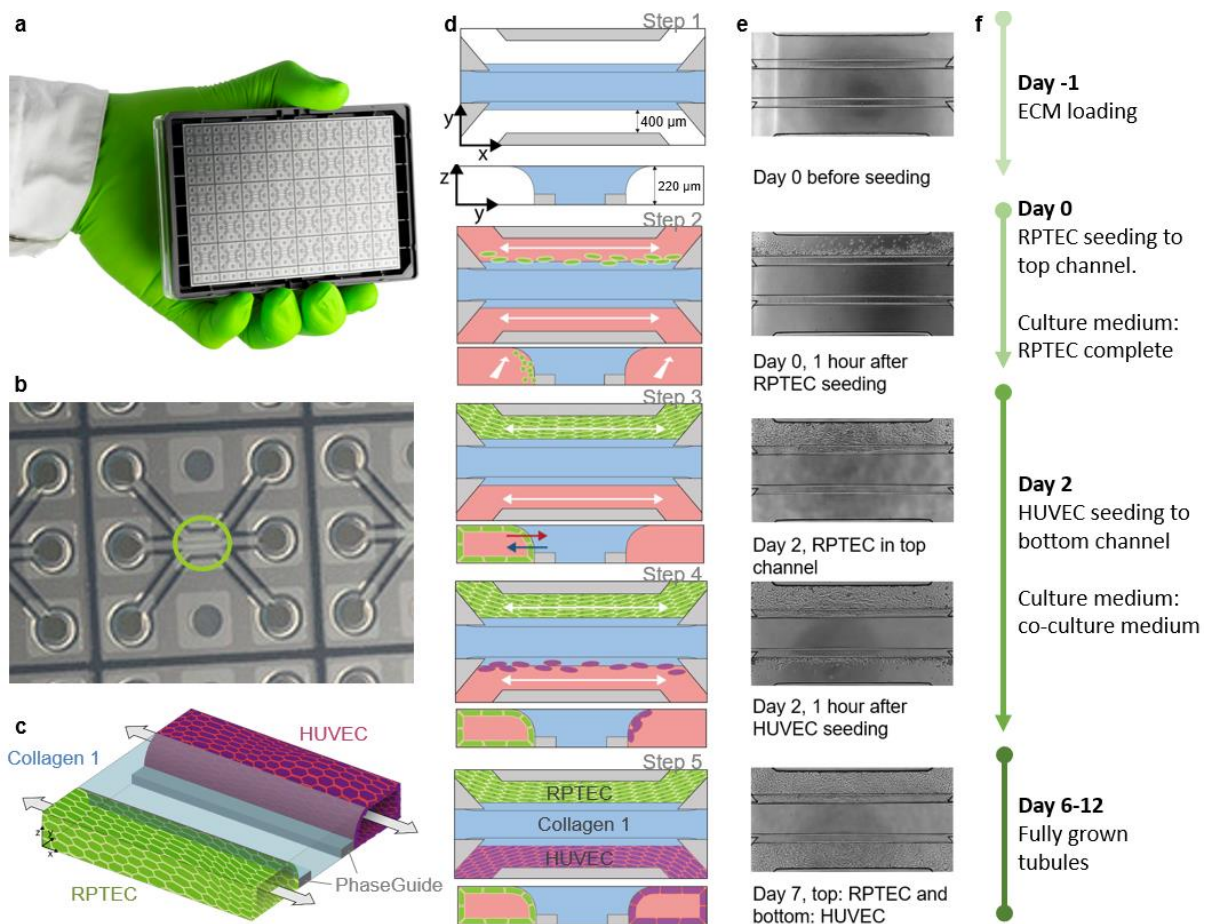


Figure 1: Overview of the seeding method of the RPTEC/HUVEC coculture in the OrganoPlate 3-lane. **a** Photograph of the bottom-side of the culture platform showing 40 microfluidic channel networks underneath a 384-well plate. **b** Zoom-in on a single microfluidic channel network comprising three channels that join in the center (green circle). **c** 3D artist impression of the center of a chip, where two tubules are cultured in the two lateral channels (green and purple) along an ECM gel in the middle channel (light blue). Two phaseguides (grey bars) define the positioning of the ECM gel leading to the three-lane stratified profile. **d** Artist impression in horizontal projection and vertical cross section, **e** associated phase-contrast images and **f** timeline for setting up the coculture. Pictures show a single chip and formation of the tubular structures at day 0, 3, and 7.

Nephrotoxicant exposure

Cultures were exposed to a concentration range of cisplatin, tobramycin and cyclosporin A (CysA) [38] (Table 1). Staurosporine (10 μM), a well-known apoptosis inducer [39], was included as a positive control, and dexamethasone (30 μM) [40] as a negative control. On day 6 medium of both channels was replaced with coculture medium complemented with a nephrotoxicant, the positive or the negative control (Table 1). Following a 48-hour incubation on the rocker platform, medium was sampled from the top wells connected to the RPTEC tubules. Samples from in- and outlet were pooled and used for the lactate dehydrogenase (LDH) activity assay. Tubules were thereafter incubated with WST-8 buffer diluted in medium to determine viability. Phase-contrast and fluorescent images were acquired using the ImageXpress XLS Micro HCl system (Molecular

Devices) to assess the morphology of the cells and their nuclei. Moreover, activation of caspase 3/7 activity was visualized.

Table 1: Nephrotoxic compounds used for validation of the model.

Compound	catalog no. (Sigma- Aldrich)	Solvent	Final vehicle conc. (v/v)	Highest concentration
Cisplatin	P4394	0.9% NaCl in H ₂ O	5.4%	270 μM
Tobramycin	T1783	Culture medium	-	50 mM
Cyclosporin A	30024	DMSO	0.6%	60 μM
Staurosporine	S4400	DMSO	0.1%	10 μM
Dexamethasone	D4902	DMSO	0.1%	30 μM

Fluorogenic caspase-3/7 assay and nuclei staining

For acquiring live cell images of cells undergoing caspase-3/7 mediated apoptosis, culture medium was replaced with medium containing Caspase-3/7 Green Apoptosis Assay Reagent (dilution 1:1000, Sartorius, #4440). After a 1.5-hour incubation at 37°C, 21% O₂, 5% CO₂ on the rocker platform a z-stack of 220 μm with 5 μm between each image plane was acquired for FITC using the ImageXpress® Micro Confocal High-Content Imaging System (Molecular Devices) with a 10x objective. The plate was thereafter fixated as described previously [24] and nuclei were stained with Hoechst 33342 and imaged again for DAPI. One maximum projection per chip was created for both, DAPI and FITC using ImageJ.

Lactate dehydrogenase activity assay

LDH activity of the samples was determined using the Lactate Dehydrogenase Activity Assay Kit (Sigma, MAK066) according to manufacturer protocol. In short, the medium of the top in- and top outlet or bottom in- and bottom outlet was pooled for RPTEC or HUVEC, respectively. 2 μL was added in duplicate to a black 384 well plate with a glass bottom. Next, 18 μL LDH assay buffer was added to all sample wells to add up to an initial volume of 20 μL. In parallel, a concentration curve of the NADH standard was added. After a short centrifugation step, 20 μL Master Reaction Mix was added to each well. After one minute, the absorbance was measured with the Multiskan™ FC Microplate Photometer (Thermo scientific) at 450 nm every 2 minutes for 6 minutes. Background subtraction was performed using the results of cell-free chips exposed to medium without any additives. The LDH activity was determined using the following formula:

$$\text{LDH activity (nmol/min/ml)} = \frac{\text{nmol NADH} \times \text{sample dilution factor}}{\text{reaction time (min)} \times \text{sample volume (mL)}}$$

Cell viability (WST-8 assay)

The viability of the cells was determined using the Cell Counting Kit – 8 (Sigma, 96992). The WST-8 solution was diluted 1:11 with coculture medium and added to both perfusion channels of one chip (30 μ L in- and outlets). After an 18-minute incubation at 37°C and 5% CO₂ on the rocker platform and a 2-minute static incubation, the absorbance in the top in- and outlets was measured with the Multiskan™ FC Microplate Photometer (Thermo scientific) at 450 nm. For background subtraction measurements from cell-free chips were used.

Modeling renal ischemia and renal reperfusion

Renal ischemia was modelled on the OrganoPlate cocultures by exposing the cultures to low oxygen (5% O₂), and/or low glucose and nutrient availability, and/or no perfusion. This was compared to a normoxic culture: atmospheric O₂ of 21%, coculture medium, and perfusion. Eight different setups were tested (Table 2).

Table 2: Conditions used to model Ischemia. N=normoxia, L=low oxygen, P=perfusion, S=static, +glu=coculture medium, -glu=DMEM w/o glucose.

Condition (abbreviation)	Oxygen Tension	Perfusion	Glucose and nutrient availability
N+P+glu	Normoxia (21% O ₂)	Yes (rocker)	Coculture medium
N+P-glu	Normoxia (21% O ₂)	Yes (rocker)	DMEM w/o glucose
N+S+glu	Normoxia (21% O ₂)	No (static)	Coculture medium
N+S-glu	Normoxia (21% O ₂)	No (static)	DMEM w/o glucose
L+P+glu	Low oxygen (5% O ₂)	Yes (rocker)	Coculture medium
L+P-glu	Low oxygen (5% O ₂)	Yes (rocker)	DMEM w/o glucose
L+S+glu	Low oxygen (5% O ₂)	No (static)	Coculture medium
L+S-glu	Low oxygen (5% O ₂)	No (static)	DMEM w/o glucose

On day 6 of the coculture, ischemic conditions were induced. For low oxygen, cultures were placed in a low oxygen incubator (5% CO₂, 37°C, 5% O₂). Perfusion was stopped by removing the plates from the rocker-platform. For low nutrient cultures the medium was changed to DMEM without glucose (Gibco #11966-025). The cultures were exposed to combinations of the ischemic conditions for 24 hours, after which medium was sampled for the LDH assay and phase-contrast images were acquired. To model renal ischemic reperfusion injury, the exposure was followed by a reperfusion of the cultures for another 24 hours in normoxic conditions. Subsequently, medium

was sampled for LDH assay, WST-8 viability was determined, phase-contrast images were acquired, and the cultures were stained for DNA and caspase-3/7 activation.

Assessment of potential protective compounds

Prevention of ischemic damage during exposure and reperfusion of the cultures was assessed upon addition of adenosine, nicotinamide and NAC during exposure and reperfusion to the culture medium of both channels (Table 3). For testing possible protecting effects of the co-incubation with the three compounds, cultures were exposed to the selected ischemic conditions L+P-glu and L+S-glu and compared to the N+P+glu control. The experiment was executed with an ischemia exposure time of 12 hours or 24 hours, both followed by 24-hour reperfusion. LDH activity samples and phase-contrast images were acquired after the exposure and after reperfusion. WST-8 viability assay and DNA and caspase-3/7 staining were performed after reperfusion only. Staurosporine (10 μ M) was used as positive control for the viability assays.

Table 3: Protective compounds tested to prevent cell damage during renal ischemia and reperfusion.

Compound	Supplier, catalog no.	Solvent	Stock conc. (mM)	Exposure conc. (mM)
Adenosine	Sigma, A4036	1M NH ₄ OH (heated) Sigma, 09859	180	1
Nicotinamide	Sigma, N0636	milliQ	1000	10
N-acetylcysteine	Sigma, A9165	milliQ	500	1

Real time imaging

On day 6 of culture, the plate was placed in the EVOS[®] FL Auto Imaging System (Life Technologies, 5% CO₂, 37°C, humidified) and incubated static in DMEM without glucose medium under 5% O₂ (L+S-glu) for 24 hours to mimic an ischemic event. Phase-contrast and FITC images were acquired every 32 minutes for 24 hours. Hereafter, the plate was reperfused with nutrient-rich coculture medium in normoxia (21% O₂) and perfusion was reinstated by placing the EVOS FL Auto Imaging System on a rocker platform (7 degree angle, 8 minute interval) for another 24-hours, while phase-contrast and FITC images were acquired every 32 minutes. During the exposure and reperfusion, cultures were co-incubated with or without 1 mM adenosine. To monitor the activation of caspase 3/7 the caspase-3/7 green apoptosis assay reagent was added to the medium (1:1000).

Data analysis and statistics

Images were processed using ImageJ [37]. Data analysis was performed using Excel (Microsoft office 365 Business) and GraphPad Prism (GraphPad Software Inc., version 8.4.2). Error bars represent the standard deviation. One-way ANOVA was used for statistical analysis between groups followed by Tukey's multiple comparisons test. A $\log(y)$ transformation was used to normalize the data if indicated by Anderson-Darling test or Brown Forsythe test of variances. In case of negative values, data was transformed using $\log(y+1)$. A p-value of < 0.05 was considered as significant.

Results

A perfused coculture of epithelial tubules and endothelial vessels was established in a microfluidic chip.

Figure 1 illustrates the setup for the perfused coculture of a human renal proximal tubule-on-a-chip and a blood vessel. RPTEC are cultured in the OrganoPlate 3-lane system against a collagen 1 ECM mimic and formed a tubular structure upon application of perfusion flow. At the same time a blood vessel was grown from HUVECs against the ECM on the other side. The 3-lane stratified setup is achieved by patterning a collagen 1 gel in the center of the chip using capillary pinning barriers called phaseguides [36].

Figure 2 shows immunohistochemical stainings of the coculture model from a top view (a, d, g) and a 3D bird's eye view (c, f, i). Tight junctions were confirmed through ZO-1 expression (Fig. 2a-f, green) [41]. Acetylated tubulin staining showed one primary cilium per cell on the luminal side for both cell types, (Fig. 2 a-c, g-i, red) [42], [43]. Epithelial marker and brush border protein Ezrin [44] was exclusively located on the apical side of the RPTEC layer (Fig. 2 d-f, red). Endothelial adherence junction protein VE-cadherin [45] was expressed by the endothelial cells at the cell borders (Fig. 2 g-i, green).

A 3D reconstruction of the coculture obtained by confocal microscopy showed that RPTEC and HUVEC adhered to the ECM in the central channel and grew to confluency after 6 and 4 days, respectively (Fig. 2 c, f, i). A view on the cross-section of both structures showed lumen formation on both sides of ECM, with the basal sides of the membranes facing each other.

The perfused 3D renal proximal tubule and blood vessel-on-a-chip is sensitive to nephrotoxicants.

Next, we assessed the response of the model to cisplatin, tobramycin, and CysA after 48-hours exposure. Phase-contrast imaging showed rounded-up and clustered cells for high concentrations of cisplatin and tobramycin, whereas the morphology of the culture upon CysA exposure remained normal for all concentrations (Fig. 3a).

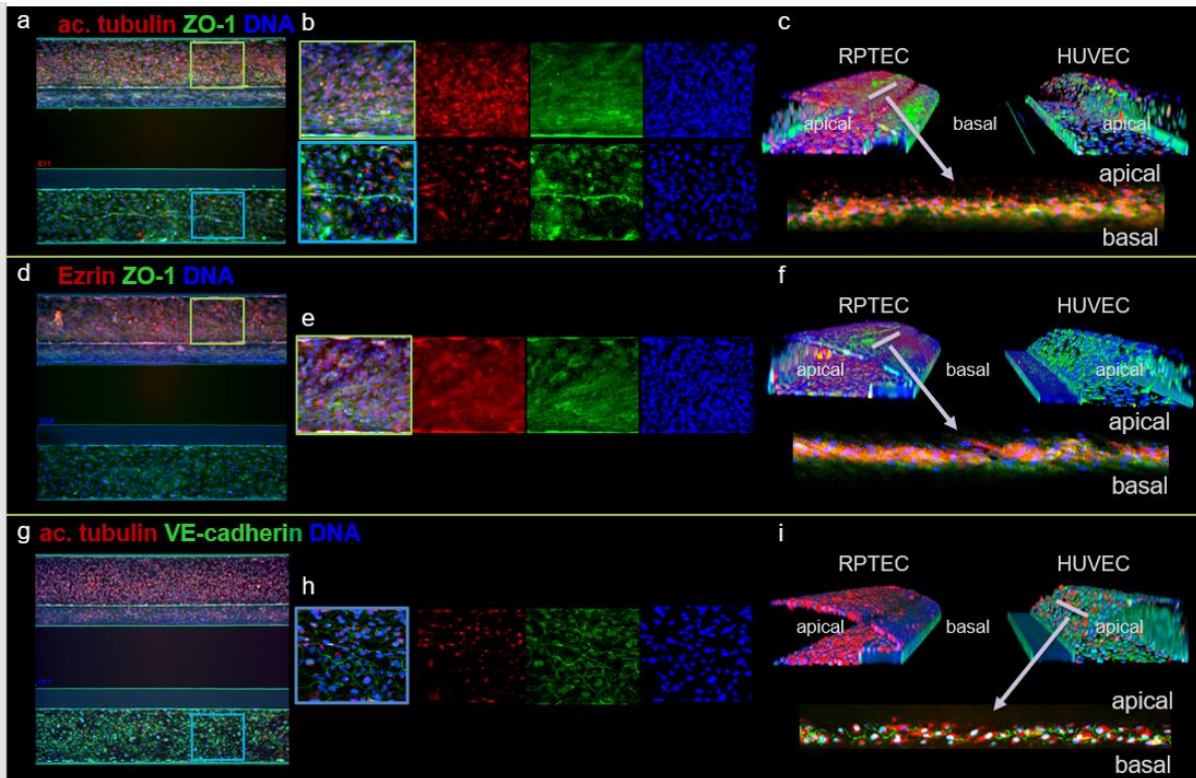


Figure 2: Marker expression of the kidney model shows polarized epithelium and endothelium. **a, d, g** z-projections of the coculture with the RPTEC tubule in the top channel and the HUVEC vessel in the bottom channel. **b, e, h** Zoom of the z-projections in **a, d, g**. **c, f, i** 3D reconstructions showing a view into the lumen of the tubules. **a-c** Primary cilia were visualized by acetylated tubulin staining (red), present on the apical side of the RPTEC tubule. Tight junction protein ZO-1 (green) was present in both cell types. **d-f** Epithelial marker and brush border protein Ezrin (red) was exclusively present on the apical side of the RPTEC tubule. **g-i** Endothelial tight junction protein VE-cadherin (green) was expressed by the HUVEC vessel at the cell border and primary cilia located on the apical side of the membrane were stained using acetylated tubulin.

DNA staining (Fig. 3b) and activated caspase 3/7 staining [46] (Fig. 3c) confirmed these observations, showing visible damage for concentration of 27 μ M cisplatin or 28.1 mM tobramycin and higher. Tubules exposed to the highest concentration of CysA showed a slight increase in the number of caspase 3/7 positive cells, though this effect was less dominant compared with the other two compounds.

LDH activity released into the medium was measured at the luminal side of RPTEC as an indicator of cell damage [47]. A trend of dose-dependent increase in LDH release was observed after treatment with cisplatin and tobramycin, whereas such a trend was not observed with CysA (Fig. 3d).

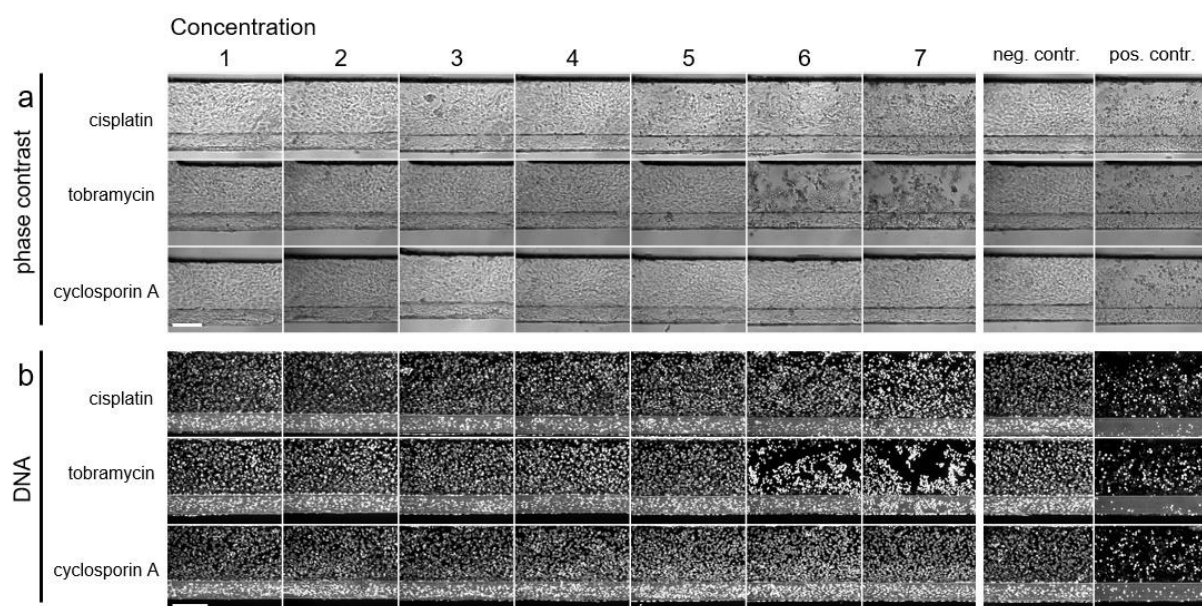
Dehydrogenase activity was measured as a representation of cell viability through a WST-8 assay (Fig. 3e, [48], [49]). Cisplatin and tobramycin exhibited a dose-dependent reduction while CysA did not affect the cell viability.

HUVEC were damaged to a similar level as RPTEC when exposed to cisplatin and tobramycin, but more severely after an exposure to CysA (data not shown). Ischemia can be induced through non-flow, low glucose and/or low oxygen.

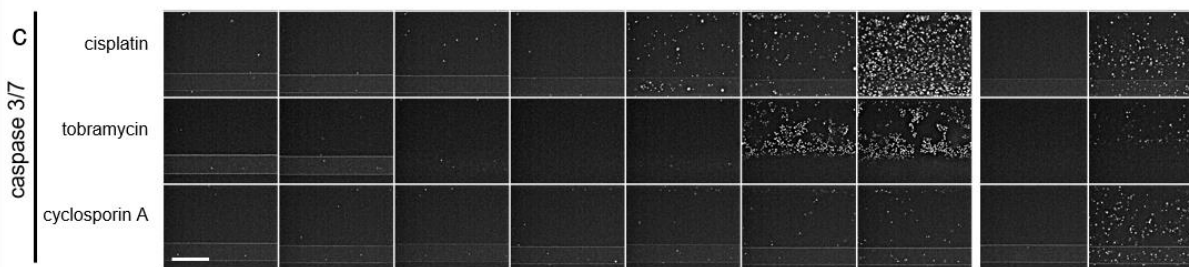
To model rIRI in the proximal tubule-on-a-chip with blood vessel, cultures were exposed to combinations of three different ischemic assaults: low oxygen (5% O₂, termed 'L'), no perfusion (static, termed 'S') and glucose free and nutrient poor medium (termed '-glu') (see Table 2 for an overview of ischemic parameter combinations). After a 24-hour exposure, cultures were reperfused under normoxic conditions (21% oxygen, termed 'N', perfusion on the rocker, termed 'P', and glucose and nutrient rich medium, (5% fetal bovine serum), termed '+glu' for another 24 hours) (Fig. 4).

Phase-contrast images of the proximal tubule after 24-hour exposure are shown in figure 4c. Among the 8 different combinations of ischemic parameters, N+S-glu, L+P-glu, and L+S-glu conditions showed rounded-up and clustered morphology. Endothelial vessels showed less severe or no damage under these conditions (S1a, top). Following the reperfusion, the damage to the proximal tubules had worsened (Fig. 4c bottom). RPTEC exposed to N+S-glu and L+S-glu were washed out of most parts of the channels during reperfusion, whereas HUVEC stayed attached even after the washing steps involved in the staining process (Fig. 4d and S1b, respectively).

Caspase 3/7 activity was determined directly after the reperfusion and showed clear activation in RPTEC when exposed to L+S-glu (Fig. 4e). A fainter staining was detected in the HUVEC in the same condition (S1c). In addition to the L+S-glu condition, caspase 3/7 activation of a few cells was detected in the L+P-glu condition in both cell types, again with a much lower activation in HUVEC.



Representative images. Scalebar = 200 μ m. Experiment 2, n=4 chips.



Representative images. Scalebar = 200 μ m. Experiment 2, n=4 chips.

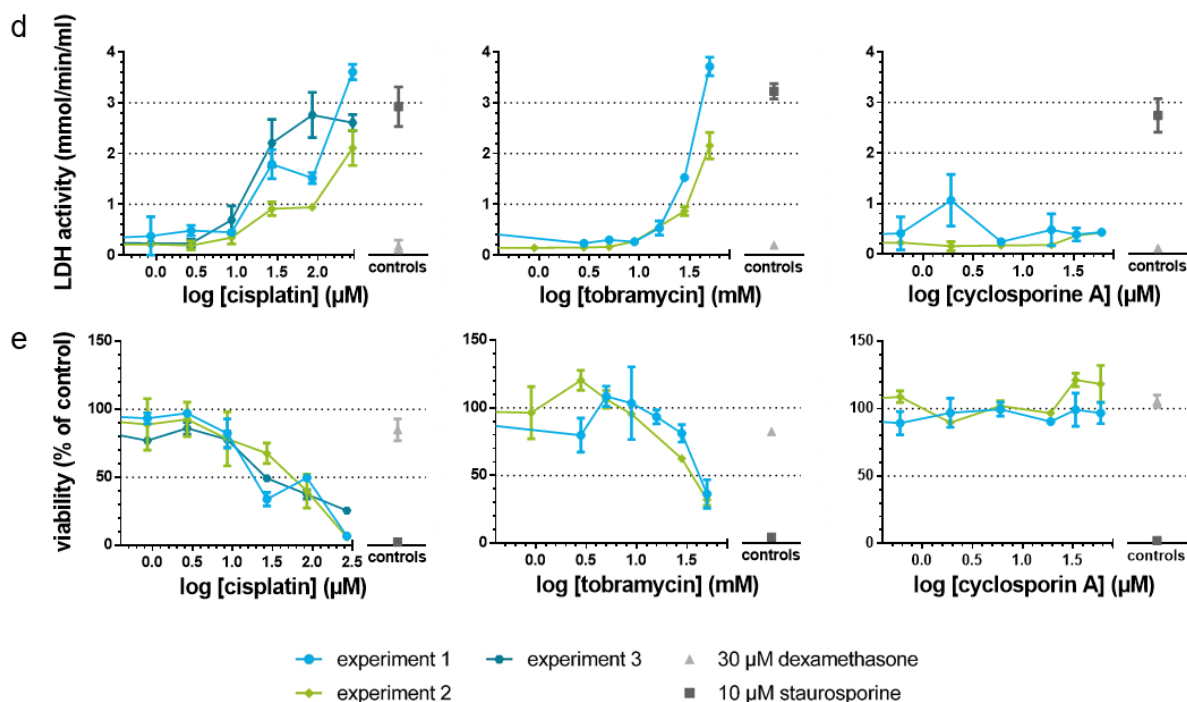


Figure 3: **A panel of assays shows susceptibility of the proximal tubule to AKI in response to nephrotoxic drugs.** Cocultures were exposed to concentrations ranges of cisplatin, tobramycin and cyclosporin A for 48 hours. **a-c** Phase-contrast imaging (a), DNA staining (b) and caspase 3/7 staining (c) showed cell damage after cisplatin and tobramycin exposure in a dose dependent manner. Representative images. Scalebar = 200 μ m. **d** LDH release in the medium was measured and showed cell damage after cisplatin and tobramycin exposure in a dose dependent manner. **e** Assessment of the viability relative to the corresponding vehicle control using a WST-8 assay showed a dose-dependent decrease in viability after cisplatin and tobramycin exposure. Dexamethasone (30 μ M) was included as a negative control, staurosporine (10 μ M) was included as a positive control. Error bars represent standard deviation. Experiment 1-3 are independent repeats of the experiment, n=2-4 chips per condition.

Figure 4f displays the LDH activity in culture medium from the RPTEC tubule after 24 hours ischemia (left panel) and subsequent reperfusion (right panel). Overall, change of LDH activity was limited in comparison to the positive control staurosporine. Under this premise, N+S-glu, L+P-glu, and L+S-glu conditions increased LDH activity, while N+P-glu condition decreased LDH activity.

After 24 hours reperfusion, N+S+glu and L+S+glu treated cultures also displayed increased LDH activity.

Assessment of the dehydrogenase activity as an index of viability showed a significant decrease of 50% in all RPTEC tubules which had been exposed to N+P-glu, N+S-glu, L+P-glu and L+S-glu. Remarkably also the cultures exposed to the condition N+P-glu showed an 50% decrease of dehydrogenase activity, which was not reflected in the LDH release. Dehydrogenase activity measured in the HUVEC cultures was 60% reduced for all conditions exposed to -glu independent from the other parameters (fig. S1).

Adenosine prevented degradation of proximal tubules under ischemic conditions.

We assessed the protective effect of adenosine, nicotinamide, and NAC in our rIRI model. Cultures were subjected to the two ischemic conditions L+P-glu and L+S-glu during 12- or 24-hour exposure, both followed by 24-hour reperfusion.

In phase-contrast imaging, obvious damage of RPTEC was observed in the L+S-glu condition after 12-hour ischemia with 24-hour reperfusion (Fig. 5a). More severe damage was observed after 24-hour ischemia with 24-hour reperfusion (Fig. 5b). Treatment with 1 mM adenosine retained RPTEC in the channel (Fig. 5 a, b, red squares), whereas disrupted RPTEC were observed when treated with 10 mM nicotinamide or 1 mM NAC. The protective effect of adenosine was confirmed by visualization of the DNA (Fig. 5 c, d). In addition, co-incubation with adenosine limited the increase of caspase 3/7 activity while in the control condition all remaining RPTEC were caspase 3/7 positive.

LDH activity in the culture medium is shown in figures 5g and 5i. Co-incubation with adenosine led to a statistically significant LDH activity reduction in four of the ischemic conditions. Unexpectedly, 10 mM nicotinamide tended to lower LDH activity at any condition including the control (Fig. 5g). We hypothesize that nicotinamide interferes with the LDH assay as nicotinamide is part of the LDH coenzyme nicotinamide-adenine dinucleotide (NAD⁺) [50] and can bind to the active site of LDH, thereby lowering the LDH activity [51]. To test this hypothesis, nicotinamide was co-incubated with staurosporine, a potent inducer of apoptosis (Fig. S3). Staurosporine exhibited renotoxicity as increase of LDH in culture media and decreased cell viability. However, co-treatment with nicotinamide decreased only LDH activity in culture media but had no influence on the WST-8 assay. This finding suggests that the LDH assay is not suitable for evaluating a renoprotective effect of nicotinamide.

Analysis of the viability by quantifying WST-8 reduction showed a decreased viability upon the ischemic event, to approximately 60% of the normoxic control condition after 12-hour exposure to L+S-glu and 35% after the exposure for 24 hours to L+S-glu. No compound appeared to be protective against ischemic damage in the WST-8 assay (Fig. 5 h, j). Results of repetition of the

experiments can be found in the supplemental figure S2. Results indicate the reproducibility of the experiments after both exposure durations, 12 and 24 hours.

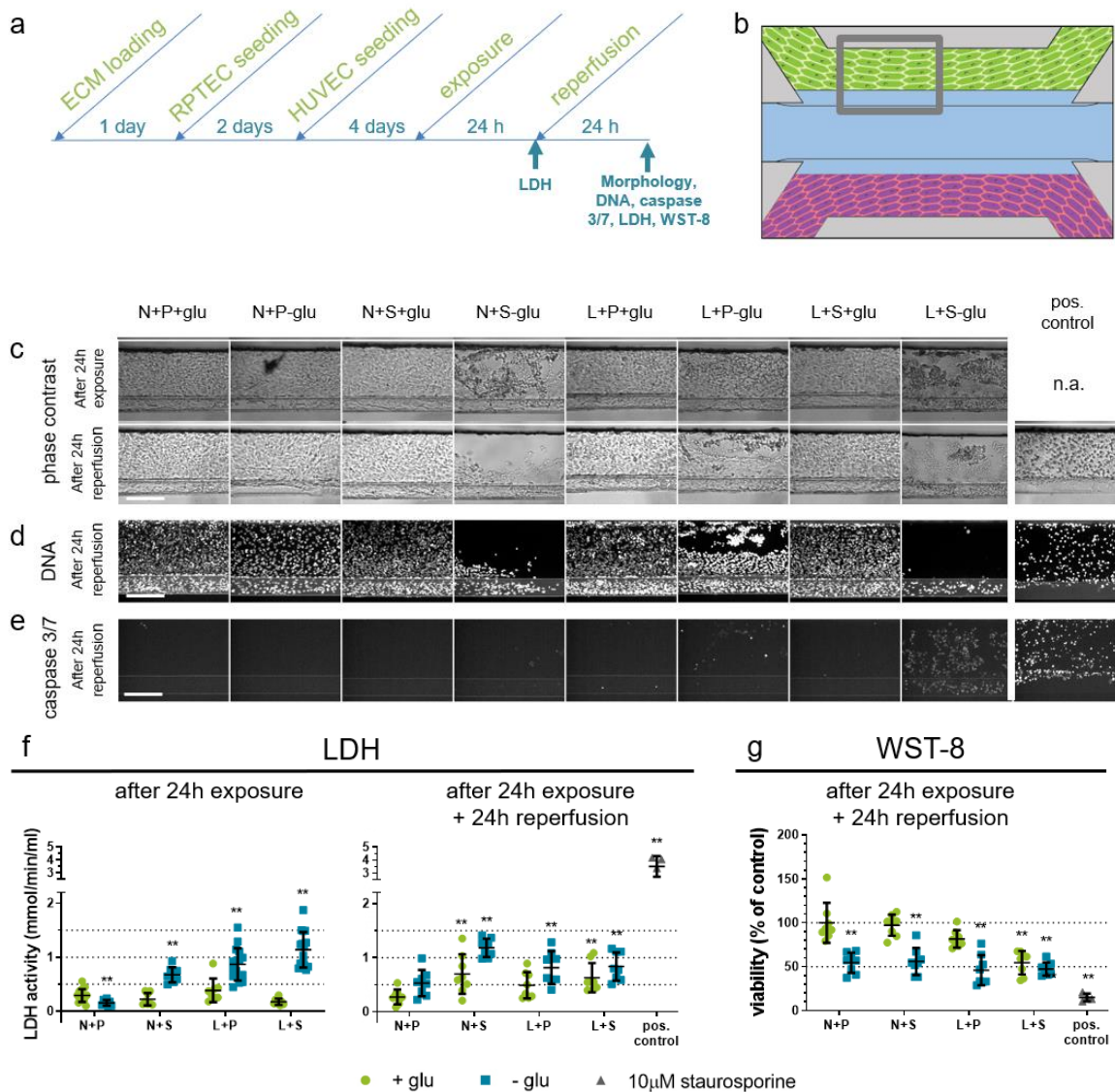


Figure 4: Ischemic conditions lead to AKI in the proximal tubule. Ischemia was modelled on the OrganoPlate coculture through a combination of low oxygen (L), static incubation (S), and glucose and nutrient poor medium (-glu) for 24-hours, followed by a 24h reperfusion in normoxia (N), perfusion on the rocker (P), and in glucose and nutrient rich medium (+glu). **a** Timeline of the experiment. **b** Region of the RPTEC tubule (GREY square) that is used for the images shown in c-e. **c** Representative phase-contrast images after 24-hour exposure (top) and subsequent 24-hour reperfusion (bottom). Different ischemia inducing conditions were tested (columns) and compared to the normal condition N+P+glu. n.a.= not available. **d** DNA staining after 24h reperfusion. **e** Caspase 3-7 staining after 24 hour reperfusion. Scalebar = 200 μ m. **f** LDH release in the medium was measured after 24 hour exposure (left) and 24 hour exposure plus 24 hour reperfusion (right) respectively. **g** WST-8 viability relative to the normal condition N+P+glu was assessed after 24h reperfusion. 10 μ M staurosporine was included as a positive control. Error bars represent standard deviation. One-way ANOVA compares the conditions to the N+P+glu control condition, ** $p < 0.01$ $n = 8-16$ chips per condition.

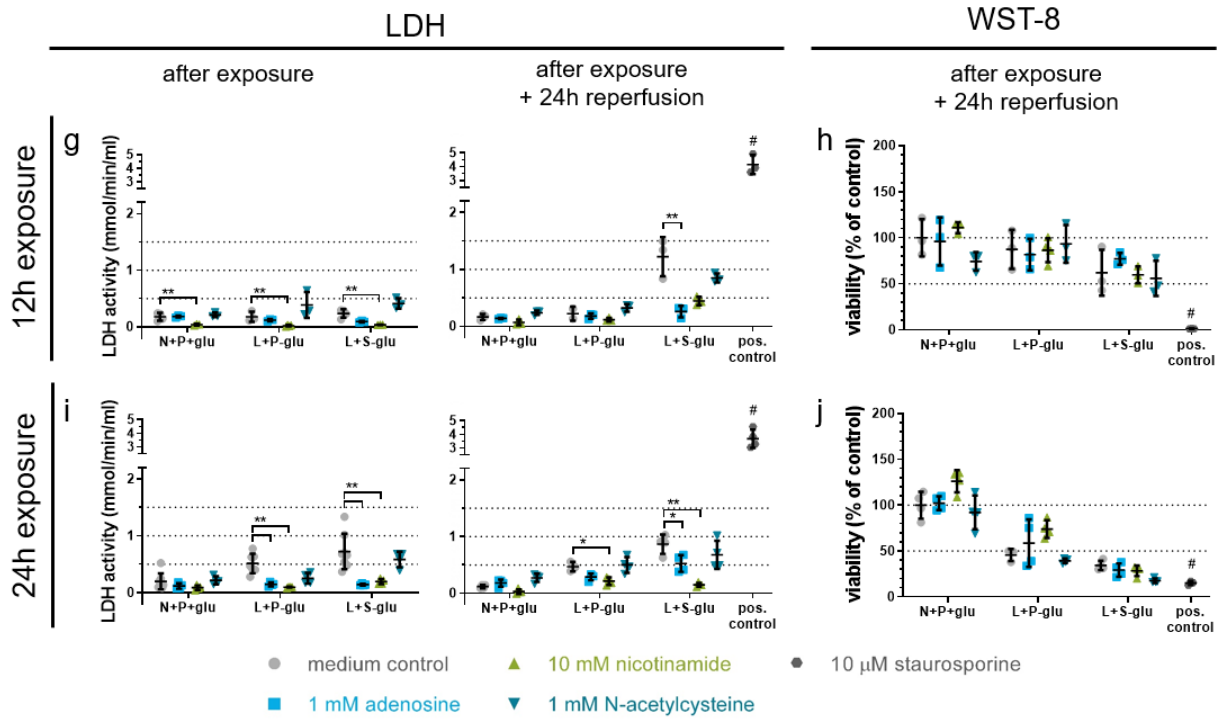
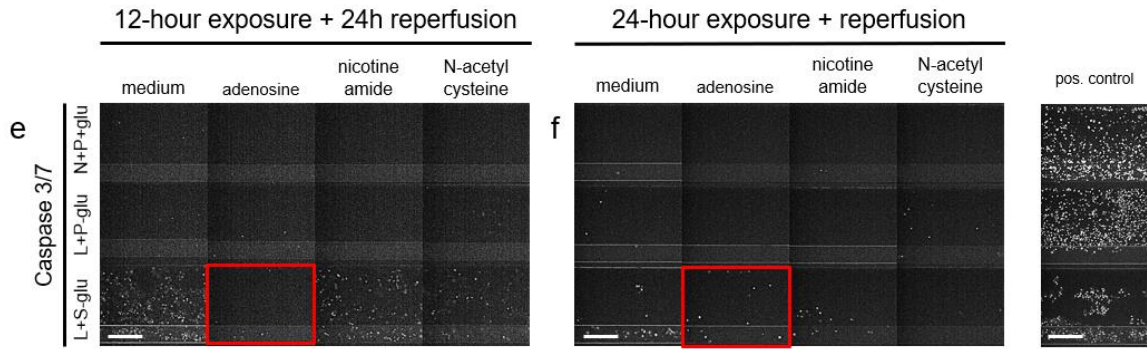
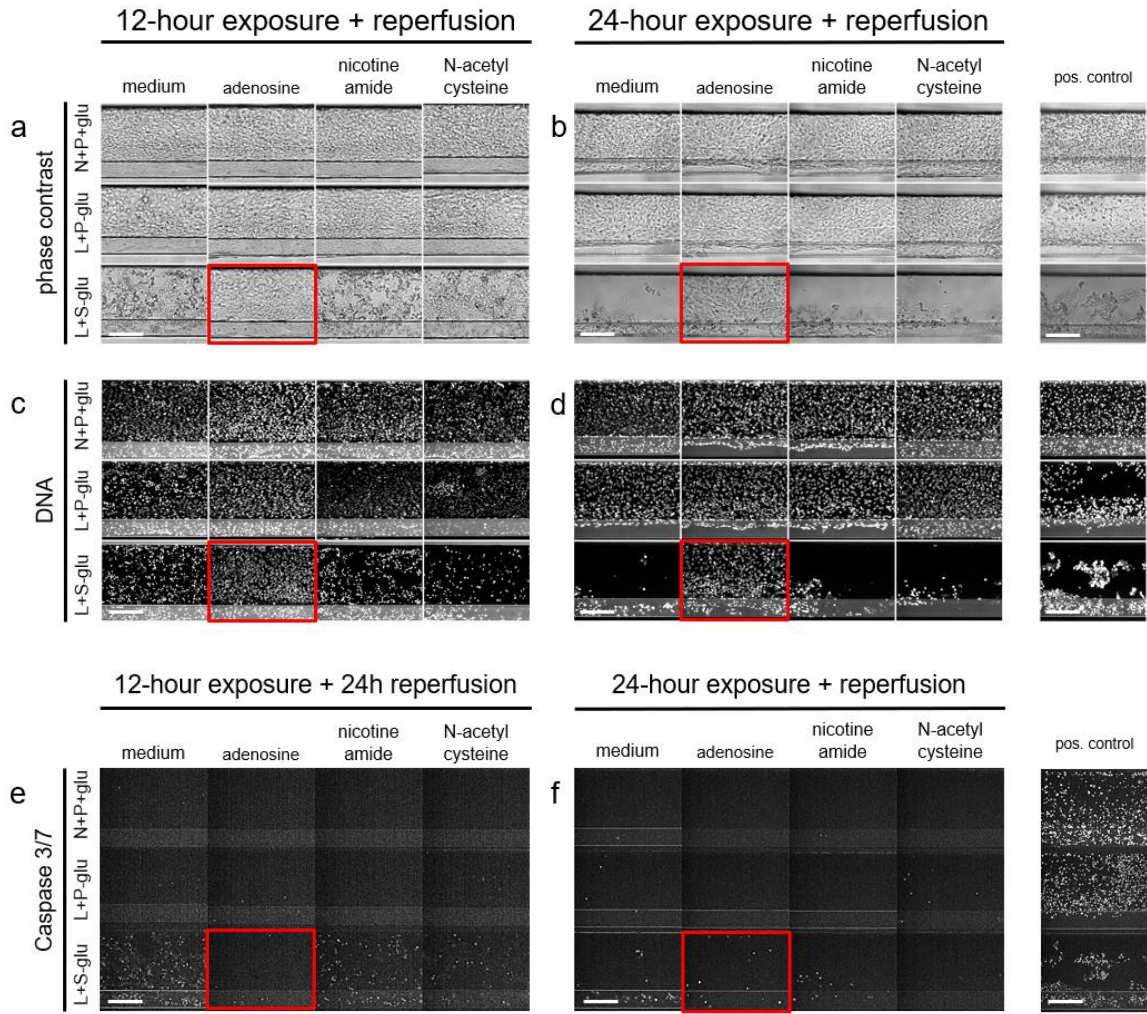


Figure 5: Co-incubation with adenosine decreases ischemia-induced AKI. Cultures were exposed to the selected ischemic conditions L+P-glu and L+S-glu for either 12 or 24 hours, followed by a 24 hour reperfusion, in the presence of adenosine, nicotinamide or N-acetylcysteine. N+P+glu medium only is the normoxic control condition. a-f Images of a region of the RPTEC tubule (see Fig. 4b) after 12-hour exposure and reperfusion (a, c, e) or after 24-hour exposure and reperfusion (b, d, f). Red squares indicate a protective effect of adenosine compared to the medium control of the same ischemic condition in phase-contrast imaging (e, f), DNA staining (g, h) and caspase 3/7 staining (i, j). Scalebar = 200µm. g-j LDH activity (g, i) and WST-8 viability relative to the N+P+glu medium control (h, j) after exposure to ischemic for 12 hours (g, h) or 24 hours (i, j) followed by reperfusion for 24 hours for both conditions. One-way ANOVA compares the co-incubations to the medium control of the same ischemic condition, * $p < 0.05$, ** $p < 0.01$. # indicates the positive control differs significantly with all medium controls ($p < 0.01$). Error bars represent the standard deviation. 10 µM staurosporine was included as a positive control. $n=3-8$ chips per condition. Both experiments (12 & 24 hour exposure) were repeated (Fig. S2).

Real time caspase 3/7 imaging confirms adenosine is protective against rIRI.

The activation of caspase 3/7 during the ischemia and reperfusion process was investigated through time-lapse fluorescent microscopy (Fig. 6, and supplemental movie).

While exposed to ischemia (L+S-glu), caspase 3/7 activity increased over time in the medium control and adenosine treated conditions (Fig. 6a). Upon reperfusion with fresh medium, severe damage to the RPTEC in the medium control was observed because of cells being washed away (Fig. 6 b, top left panel), whereas proximal tubules treated with adenosine remained (Fig. 6b top right panel). After 12 and 24 hours of the reperfusion process, detached RPTEC, as well as an increase of activated caspase 3/7 in the remaining RPTEC, were observed in the medium control, while there were no severely disturbed RPTEC observed with adenosine treatment. HUVEC vessels recovered from the ischemic event, independent of adenosine co-incubation.

Discussion

In this study, we presented a human renal proximal tubule-on-a-chip in coculture with a perfused blood vessel separated by an ECM with the purpose to model rIRI-induced AKI (Fig. 1). A 3D reconstruction of histochemical stainings of the cocultures obtained by confocal microscopy showed that RPTEC and HUVEC adhere to the ECM and the side walls in the shape of tubular/vessel structures with lumen formation (Fig. 2). Correct polarization of the RPTEC was shown by a staining against the brush border marker ezrin. Primary cilia labeled with acetylated tubulin were observed on the apical surface of RPTEC and ZO-1, which is a key molecule of tight junctions, was found at the borders of the cells. Consistent with prior work [24] RPTEC formed barriers with limited diffusion of large molecules such as fluorescein labeled dextran (4.4 kDa and 150 kDa; data not shown) suggesting that the barrier function is well maintained. While this model is used in the present study, there is abundant room for further modifications. For instance, immune cells could be added to the lumen of the endothelial vessel, allowing the investigation of

translocation of immune cells by the endothelium, and their role in inflammation of the kidney microenvironment.

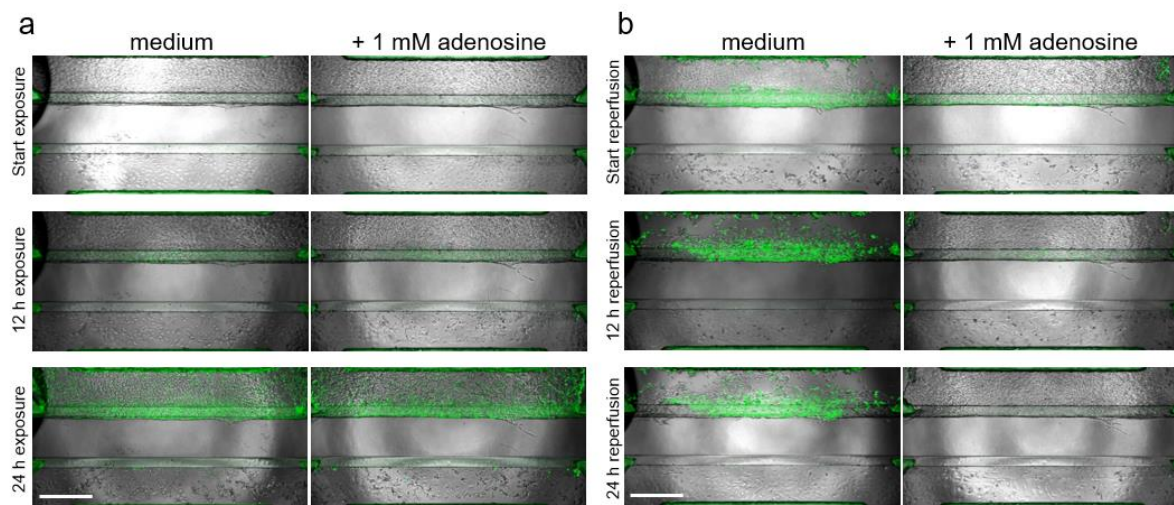


Figure 6: Real time caspase 3/7 activation and phase contrast imaging shows protective effect of adenosine upon ischemic exposure. a Cultures, co-incubated with and without 1 mM adenosine were exposed to ischemic conditions (L+S-glu) for 24 hours and caspase 3/7 activity was monitored over time. **b** Medium was refreshed to standard culture medium and cocultures were reperfused under normal conditions (N+P+glu) for 24 hours. Green = activated caspase 3/7. Scalebar = 500 μ m. Representative images of $n=3$ chips per condition. A corresponding time lapse movie can be viewed in the supplemental movie.

To apply this new culture setup to *in vitro* AKI disease modeling, the response of the model to several renotoxicants was tested and the feasibility to measure cellular damage was assessed using several assays. Cisplatin, tobramycin, and CysA were capable to affect RPTEC in the advanced model as shown in figure 3. Tobramycin is an aminoglycoside antibiotic which causes nephrotoxicity in clinical settings [52]. Our model detected its toxicity from 28.1 mM, which is higher than concentrations used clinically (around 2 μ g/mL) [52]. In clinical settings, nephrotoxicity of tobramycin is observed after multiple ingestions [52], while in the present study tobramycin exposure was performed at a single dosing for 48 hours. Using a longer time frame with repeated dosing a toxic effect might be detected at lower concentrations. CysA treatment resulted in increased caspase 3/7 activity at 60 μ M. Li et al [53] reported caspase 3/7 activation by CysA with an EC50 of 11 μ M in a two-dimensional culture setting of the same cell source (RPTEC SA7K clone). It would be interesting to compare the expression levels of P-glycoprotein, a ABC-transporter, between these culture settings as CysA is a substrate of P-glycoprotein [54]. Different levels could potentially cause a change of the intracellular concentration of CysA. In conclusion, all assays were suitable to detect reasonable cellular responses and we decided to use the model for disease modeling of rIRI.

We modelled an ischemic event on the kidney-on-a-chip by exposing the culture to a combination of three ischemic parameters: low oxygen (5%) (L), no perfusion (S), nutrient/glucose-poor medium (-glu), and combinations of the three. After exposure, reperfusion was reinstated under normal conditions (N+P+glu). When exposed to combined culture conditions (summarized in Table 2), N+S-glu, L+P-glu, and L+S-glu led to damage after the 24-hour exposure followed the reperfusion (Fig. 4). A significant change was observed in tubular morphology: cells appeared as rounded and detached cells were observed. Moreover, increased caspase 3/7 activity was observed in remaining epithelial cells after ischemia-reperfusion (L+S-glu or L+P-glu). These observations are in line with clinical observations as the loss of the brush border and detached epithelium were reported to be found in biopsy samples from AKI patients [8].

We investigated the potential renoprotective effects of adenosine, nicotinamide, and NAC when co-treated during the rIRI event of the two selected ischemic conditions L+P-glu and L+S-glu. A protective effect of the co-incubation with adenosine was observed in the morphology and DNA assessment, caspase 3/7 activation, and LDH release. However, dehydrogenase activity measured with the WST-8 viability assay showed no effect of adenosine. Based on these results we hypothesize that adenosine exerts its protection by lowering the cell metabolism [55], including the dehydrogenase activity. By putting the cells in a resting phase with low metabolism, the oxygen demand of the cells is minimal, which could prevent damage from ischemic condition. Overall, our results suggest that adenosine protects death of RPTEC through reduction of caspase 3/7 activation.

In contrast to adenosine, NAC did not show a renoprotective effect. There are positive reports of NAC being protective in animal rIRI models. Our observation that we did not see a protective effect in our human rIRI model could point towards a species-to-species difference, and that NAC in fact does not have a protective effect in humans. In fact, the KDIGO Clinical Practice Guideline for AKI [56] does not recommend using NAC for prevention of postsurgical AKI. We recommend follow-up research to further validate this hypothesis.

Nicotinamide is one of the precursors of nicotinamide adenine dinucleotide (NAD⁺), lately considered for its therapeutic potential as an NAD booster [57]. Recently, results of a phase 1 pilot study administering nicotinamide was reported [31], [58]. In patients undergoing cardiac surgery, an increase of precursors for NAD⁺ was observed in their serum and urine accompanied by a decrease of serum creatinine. In contrast to our expectations, nicotinamide did not prevent tubular damage in our *in vitro* rIRI model. A decrease of LDH activity after nicotinamide treatment, was contributed to the interference of nicotinamide with the assay as described in result section. Follow-up studies will also help to better understand the translatability of this model to humans. In this regard, time-lapse imaging (Fig. 6 and supplemental movie) can be a powerful tool for monitoring the changes of cellular appearance. We selected a 12-hour or 24-hour duration for mimicking the ischemic exposure, while this duration might be too long to observe the

renoprotective effect of nicotinamide. Further assay optimization facilitated by such live imaging should be undertaken to investigate a broader range of various ischemic conditions and treatments at multiple evaluation time-points.

Endothelium seemed to be more tolerant to ischemia compared to the epithelium, and showed recovery during reperfusion, independent of the treatment condition (Figs. 4 and 6, Fig. S2). Further investigation will be needed to investigate the effect of rIRI on endothelial cells including further readouts such as endothelial marker expression, barrier integrity of the endothelial cell layer, and release of cytokines.

In an earlier study, it was shown that glomerular specific endothelium is key to mimic specific aspects of the glomerulus, including glomerular specific extracellular matrix components [59]. We therefore expect that translatability of our model could be further increased by replacing HUVEC with endothelial cells of the kidney. Alternatively, inclusion of induced pluripotent stem cell-derived cells could be done to study different genetic backgrounds and predispositions. We also anticipate of usage of urine derived tubuloids [60] to capture patient specific responses to ischemic events.

The current model is sufficiently robust to push forward to a high throughput phenotypic screen for finding novel protective compounds that protect the kidney during ischemia and reperfusion. The OrganoPlate platform used in this study is compatible, next to general laboratory equipment, with high content (fluorescent) microscopes and robotics. Kane *et al.* have already reported automation of the system for neuronal cultures [61]. Importantly, we showed that we could measure response to these effects with various orthogonal assays. This allows internal hit verification in a single run.

In conclusion, we successfully expanded our human renal proximal tubule-on-a-chip to a coculture setting with endothelial cells. We were able to study the effect of ischemic conditions and their role in AKI induction by adjustment of various culture settings (nutrient composition, oxygen tension, and perfusion flow). We found that ischemic conditions had a strong detrimental effect on the proximal tubule, but only mildly impacted the endothelium. We furthermore confirmed that adenosine had a protective effect. We thus conclude that we have established a powerful platform to study AKI *in vitro* that will prove useful to advance our understanding of the pathophysiological nature of rIRI and support development of novel therapies for preventing AKI.

Author contributions

Conception and design: MK Vormann, M Ohbuchi, F Kiyonaga, HL Lanz, K Tetsuka

Acquisition of data: MK Vormann, LM Tool, L Gijzen

Analysis and interpretation of data: MK Vormann, LM Tool, M Ohbuchi, R van Vught, T Hankemeier, F Kiyonaga, T Kawabe, T Goto, A Fujimori, HL Lanz, K Tetsuka

Supervision: P Vulto, HL Lanz, K Tetsuka

Drafting the manuscript: MK Vormann, HL Lanz, P Vulto, K Tetsuka

Revising the manuscript: All authors commented on the draft manuscript.

Acknowledgements, Disclosures, and Funding:

MK Vormann, LM Tool, L Gijzen, R van Vught, P Vulto, and HL Lanz are employees of MIMETAS BV, the Netherlands, which is marketing the OrganoPlate. P Vulto and T Hankemeier are shareholders of that same company. OrganoPlate is a trademark of MIMETAS BV. This research project was supported through funding from Astellas Pharma Inc.

References

- [1] A. Zuk and J. V. Bonventre, "Acute Kidney Injury," *Annu. Rev. Med.*, vol. 67, no. 1, pp. 293–307, Jan. 2016, doi: 10.1146/annurev-med-050214-013407.
- [2] A. J. P. Lewington, J. Cerdá, and R. L. Mehta, "Raising awareness of acute kidney injury: a global perspective of a silent killer," *Kidney Int.*, vol. 84, no. 3, pp. 457–467, Sep. 2013, doi: 10.1038/ki.2013.153.
- [3] D. P. Basile, M. D. Anderson, and T. A. Sutton, "Pathophysiology of acute kidney injury," *Compr. Physiol.*, vol. 2, no. 2, pp. 1303–1353, 2012, doi: 10.1002/cphy.c110041.
- [4] M. A. Perazella, "Renal vulnerability to drug toxicity," *Clin. J. Am. Soc. Nephrol.*, vol. 4, no. 7, pp. 1275–1283, 2009, doi: 10.2215/CJN.02050309.
- [5] S. P. Soltoff, "ATP and the Regulation of Renal Cell Function," *Annu. Rev. Physiol.*, vol. 48, no. 1, pp. 9–31, Oct. 1986, doi: 10.1146/annurev.ph.48.030186.000301.
- [6] P. Hansell, W. J. Welch, R. C. Blantz, and F. Palm, "Determinants of kidney oxygen consumption and their relationship to tissue oxygen tension in diabetes and hypertension," *Clin. Exp. Pharmacol. Physiol.*, vol. 40, no. 2, pp. 123–137, 2013, doi: 10.1111/1440-1681.12034.
- [7] K. Makris and L. Spanou, "Acute Kidney Injury: Definition, Pathophysiology and Clinical Phenotypes," *Clin. Biochem. Rev.*, vol. 37, no. 2, pp. 85–98, 2016, [Online]. Available: <https://www.ncbi.nlm.nih.gov/pmc/articles/PMC5198510/>.
- [8] J. V Bonventre and L. Yang, "Cellular pathophysiology of ischemic acute kidney injury," *J. Clin. Invest.*, vol. 121, no. 11, pp. 4210–4221, Nov. 2011, doi: 10.1172/JCI45161.
- [9] M. Malek and M. Nematbakhsh, "Renal ischemia/reperfusion injury; from pathophysiology to treatment.," *J. Ren. Inj. Prev.*, vol. 4, no. 2, pp. 20–27, 2015, doi: 10.12861/jrip.2015.06.
- [10] G. R. Kinsey, L. Li, and M. D. Okusa, "Inflammation in acute kidney injury," *Nephron - Exp. Nephrol.*, vol. 109, no. 4, 2008, doi: 10.1159/000142934.
- [11] M. K. Nadim *et al.*, "COVID-19-associated acute kidney injury: consensus report of the 25th Acute Disease Quality Initiative (ADQI) Workgroup," *Nat. Rev. Nephrol.*, Oct. 2020, doi: 10.1038/s41581-020-00356-5.
- [12] W. Lieberthal and S. K. Nigam, "Acute renal failure. II. Experimental models of acute renal

- failure: imperfect but indispensable," *Am. J. Ren. Physiol.*, vol. 278, no. 1, pp. F1–F12, 2000.
- [13] N. I. Skrypnik, L. J. Siskind, S. Faube, and M. P. de Caestecker, "Bridging translation for acute kidney injury with better preclinical modeling of human disease," *Am. J. Physiol. - Ren. Physiol.*, vol. 310, no. 10, pp. F972–F984, 2016, doi: 10.1152/ajprenal.00552.2015.
- [14] A. L. Russ, K. M. Haberstroh, and A. E. Rundell, "Experimental strategies to improve *in vitro* models of renal ischemia," *Exp. Mol. Pathol.*, vol. 83, no. 2, pp. 143–159, 2007, doi: 10.1016/j.yexmp.2007.03.002.
- [15] V. van Duinen, S. J. Trietsch, J. Joore, P. Vulto, and T. Hankemeier, "Microfluidic 3D cell culture: From tools to tissue models," *Curr. Opin. Biotechnol.*, vol. 35, pp. 118–126, 2015, doi: 10.1016/j.copbio.2015.05.002.
- [16] M. J. Wilmer, C. P. Ng, H. L. Lanz, P. Vulto, L. Suter-Dick, and R. Masereeuw, "Kidney-on-a-Chip Technology for Drug-Induced Nephrotoxicity Screening," *Trends Biotechnol.*, vol. 34, no. 2, pp. 156–170, 2016, doi: 10.1016/j.tibtech.2015.11.001.
- [17] G. A. Van Norman, "Limitations of Animal Studies for Predicting Toxicity in Clinical Trials: Is it Time to Rethink Our Current Approach?," *JACC Basic to Transl. Sci.*, vol. 4, no. 7, pp. 845–854, 2019, doi: 10.1016/j.jacbts.2019.10.008.
- [18] U. Marx *et al.*, "Biology-inspired microphysiological systems to advance patient benefit and animal welfare in drug development," *ALTEX*, vol. 37, no. 3, pp. 364–394, 2020, doi: 10.14573/altex.2001241.
- [19] K. Tetsuka *et al.*, "Reconstituted human organ models as a translational tool for human organ response: Definition, expectations, cases, and strategies for implementation in drug discovery and development," *Biol. Pharm. Bull.*, vol. 43, no. 3, pp. 375–383, 2020, doi: 10.1248/bpb.b19-01070.
- [20] S. G. Lloyd, P. Wang, H. Zeng, and J. C. Chatham, "Impact of low-flow ischemia on substrate oxidation and glycolysis in the isolated perfused rat heart," *Am. J. Physiol. - Hear. Circ. Physiol.*, vol. 287, no. 1 56-1, 2004, doi: 10.1152/ajpheart.00983.2003.
- [21] K. J. Jang *et al.*, "Human kidney proximal tubule-on-a-chip for drug transport and nephrotoxicity assessment," *Integr. Biol. (United Kingdom)*, vol. 5, no. 9, pp. 1119–1129, 2013, doi: 10.1039/c3ib40049b.
- [22] J. Jansen *et al.*, "Human proximal tubule epithelial cells cultured on hollow fibers: Living membranes that actively transport organic cations," *Sci. Rep.*, vol. 5, no. November, pp. 1–12, 2015, doi: 10.1038/srep16702.
- [23] K. A. Homan *et al.*, "Bioprinting of 3D Convuluted Renal Proximal Tubules on Perfusable Chips," *Sci. Rep.*, vol. 6, pp. 1–13, 2016, doi: 10.1038/srep34845.
- [24] M. K. Vormann *et al.*, "Nephrotoxicity and Kidney Transport Assessment on 3D Perfused Proximal Tubules," *AAPS J.*, vol. 20, no. 5, pp. 1–11, 2018, doi: 10.1208/s12248-018-0248-z.
- [25] Y. Duan *et al.*, "Shear-induced reorganization of renal proximal tubule cell actin cytoskeleton and apical junctional complexes," *Proc. Natl. Acad. Sci. U. S. A.*, vol. 105, no. 32, pp. 11418–11423, 2008, doi: 10.1073/pnas.0804954105.
- [26] V. Raghavan, Y. Rbaibi, N. M. Pastor-Soler, M. D. Carattino, and O. A. Weisz, "Shear stress-

dependent regulation of apical endocytosis in renal proximal tubule cells mediated by primary cilia," *Proc. Natl. Acad. Sci. U. S. A.*, vol. 111, no. 23, pp. 8506–8511, 2014, doi: 10.1073/pnas.1402195111.

- [27] S. Weinbaum, Y. Duan, L. M. Satlin, T. Wang, and A. M. Weinstein, "Mechanotransduction in the renal tubule," *Am. J. Physiol. - Ren. Physiol.*, vol. 299, no. 6, pp. 1220–1236, 2010, doi: 10.1152/ajprenal.00453.2010.
- [28] A. A. McDonough, "Mechanisms of proximal tubule sodium transport regulation that link extracellular fluid volume and blood pressure," *Am. J. Physiol. Integr. Comp. Physiol.*, vol. 298, no. 4, pp. R851–R861, Apr. 2010, doi: 10.1152/ajpregu.00002.2010.
- [29] J. Vriend *et al.*, "Screening of Drug-Transporter Interactions in a 3D Microfluidic Renal Proximal Tubule on a Chip," *AAPS J.*, vol. 20, no. 5, 2018, doi: 10.1208/s12248-018-0247-0.
- [30] L. Suter-Dick *et al.*, "Combining Extracellular miRNA Determination with Microfluidic 3D Cell Cultures for the Assessment of Nephrotoxicity: a Proof of Concept Study," *AAPS J.*, vol. 20, no. 5, pp. 1–9, 2018, doi: 10.1208/s12248-018-0245-2.
- [31] A. Poyan Mehr *et al.*, "De novo NAD⁺ biosynthetic impairment in acute kidney injury in humans," *Nat. Med.*, vol. 24, no. 9, pp. 1351–1359, 2018, doi: 10.1038/s41591-018-0138-z.
- [32] A. C. Seguro, L. F. Poli De Figueiredo, and M. H. M. Shimizu, "N-acetylcysteine (NAC) protects against acute kidney injury (AKI) following prolonged pneumoperitoneum in the rat," *J. Surg. Res.*, vol. 175, no. 2, pp. 312–315, 2012, doi: 10.1016/j.jss.2011.05.052.
- [33] M. H. M. Shimizu *et al.*, "N-acetylcysteine protects against renal injury following bilateral ureteral obstruction," *Nephrol. Dial. Transplant.*, vol. 23, no. 10, pp. 3067–3073, Jun. 2008, doi: 10.1093/ndt/gfn237.
- [34] T. M. DesRochers, L. Suter, A. Roth, and D. L. Kaplan, "Bioengineered 3D Human Kidney Tissue, a Platform for the Determination of Nephrotoxicity," *PLoS One*, vol. 8, no. 3, 2013, doi: 10.1371/journal.pone.0059219.
- [35] H. T. Lee and C. W. Emala, "Protective effects of renal ischemic preconditioning and adenosine pretreatment: Role of A1 and A3 receptors," *Am. J. Physiol. - Ren. Physiol.*, vol. 278, no. 3 47-3, pp. 380–387, 2000, doi: 10.1152/ajprenal.2000.278.3.f380.
- [36] P. Vulto, S. Podszun, P. Meyer, C. Hermann, A. Manz, and G. A. Urban, "Phaseguides: A paradigm shift in microfluidic priming and emptying," *Lab Chip*, vol. 11, no. 9, pp. 1596–1602, 2011, doi: 10.1039/c0lc00643b.
- [37] J. Schindelin *et al.*, "Fiji: An open-source platform for biological-image analysis," *Nat. Methods*, vol. 9, no. 7, pp. 676–682, 2012, doi: 10.1038/nmeth.2019.
- [38] S. Raju, S. Kavimani, V. Uma Maheshwara Rao, and K. Sriramulu Reddy, "Nephrotoxicants and nephrotoxicity testing: An outline of *In vitro* alternatives," *J. Pharm. Sci. Res.*, vol. 3, no. 3, pp. 1110–1116, 2011.
- [39] C. A. Belmokhtar, J. Hillion, and E. Ségal-Bendirdjian, "Staurosporine induces apoptosis through both caspase-dependent and caspase-independent mechanisms," *Oncogene*, vol. 20, no. 26, pp. 3354–3362, 2001, doi: 10.1038/sj.onc.1204436.
- [40] K. A. Jacob *et al.*, "Intraoperative high-dose dexamethasone and severe AKI after cardiac

- surgery," *J. Am. Soc. Nephrol.*, vol. 26, no. 12, pp. 2947–2951, 2015, doi: 10.1681/ASN.2014080840.
- [41] B. R. Stevenson, J. D. Siliciano, M. S. Mooseker, and D. A. Goodenough, "Identification of ZO-1: A high molecular weight polypeptide associated with the tight junction (Zonula Occludens) in a variety of epithelia," *J. Cell Biol.*, vol. 103, no. 3, pp. 755–766, 1986, doi: 10.1083/jcb.103.3.755.
- [42] A. D. Egorova, K. van der Heiden, R. E. Poelmann, and B. P. Hierck, "Primary cilia as biomechanical sensors in regulating endothelial function," *Differentiation*, vol. 83, no. 2, pp. S56–S61, 2012, doi: 10.1016/j.diff.2011.11.007.
- [43] V. Raghavan and O. A. Weisz, "Flow stimulated endocytosis in the proximal tubule," *Curr. Opin. Nephrol. Hypertens.*, vol. 24, no. 4, pp. 359–365, 2015, doi: 10.1097/MNH.000000000000135.
- [44] M. Berryman, Z. Franck, and A. Bretscher, "Ezrin is concentrated in the apical microvilli of a wide variety of epithelial cells whereas moesin is found primarily in endothelial cells," *J. Cell Sci.*, vol. 105, no. 4, pp. 1025–1043, 1993.
- [45] M. Giannotta, M. Trani, and E. Dejana, "Review VE-Cadherin and Endothelial Adherens Junctions : Active Guardians of Vascular Integrity," *Dev. Cell*, vol. 26, no. 5, pp. 441–454, 2013, doi: 10.1016/j.devcel.2013.08.020.
- [46] K. M. Hanson and J. N. Finkelstein, "An accessible and high-throughput strategy of continuously monitoring apoptosis by fluorescent detection of caspase activation," *Anal. Biochem.*, vol. 564–565, no. September 2018, pp. 96–101, 2019, doi: 10.1016/j.ab.2018.10.022.
- [47] C. Legrand *et al.*, "Lactate dehydrogenase (LDH) activity of the number of dead cells in the medium of cultured eukaryotic cells as marker," *J. Biotechnol.*, vol. 25, no. 3, pp. 231–243, 1992, doi: 10.1016/0168-1656(92)90158-6.
- [48] H. Tominaga *et al.*, "A water-soluble tetrazolium salt useful for colorimetric cell viability assay," *Anal. Commun.*, vol. 36, no. 2, pp. 47–50, 1999, doi: 10.1039/a809656b.
- [49] K. Chamchoy, D. Pakotiprapha, P. Pumirat, U. Leartsakulpanich, and U. Boonyuen, "Application of WST-8 based colorimetric NAD(P)H detection for quantitative dehydrogenase assays," *BMC Biochem.*, vol. 20, no. 1, pp. 1–14, 2019, doi: 10.1186/s12858-019-0108-1.
- [50] A. McPherson, "Interaction of lactate dehydrogenase with its coenzyme, nicotinamide-adenine dinucleotide," *J. Mol. Biol.*, vol. 51, no. 1, pp. 39–46, 1970, doi: 10.1016/0022-2836(70)90268-8.
- [51] A. J. Forlano, "Effect of the component parts of nicotinamide adenine dinucleotide (NAD \oplus) as inhibitors of lactic dehydrogenase," *J. Pharm. Sci.*, vol. 56, no. 6, pp. 763–5, 1967.
- [52] F. Paquette *et al.*, "Acute Kidney Injury and Renal Recovery with the Use of Aminoglycosides: A Large Retrospective Study," *Nephron*, vol. 131, no. 3, pp. 153–160, 2015, doi: 10.1159/000440867.
- [53] S. Li *et al.*, "Development and Application of Human Renal Proximal Tubule Epithelial Cells for Assessment of Compound Toxicity," *Curr. Chem. Genomics Transl. Med.*, vol. 11, no. 1, pp. 19–30, Feb. 2017, doi: 10.2174/2213988501711010019.

- [54] T. Saeki, K. Ueda, Y. Tanigawara, R. Hori, and T. Komano, "Human P-glycoprotein transports cyclosporin A and FK506," *J. Biol. Chem.*, vol. 268, no. 9, pp. 6077–6080, 1993.
- [55] S. C. Yap and H. Thomas Lee, "Adenosine and protection from acute kidney injury," *Curr. Opin. Nephrol. Hypertens.*, vol. 21, no. 1, pp. 24–32, 2012, doi: 10.1097/MNH.0b013e32834d2ec9.
- [56] Acute Kidney Injury Work Group. KDIGO Clinical Practice Guideline for Acute Kidney Injury, "Kidney Disease: Improving Global Outcomes (KDIGO)," *Kidney Int. Suppl.*, vol. 2, pp. 1–138, Mar. 2012, doi: 10.1038/kisup.2012.1.
- [57] L. Rajman, K. Chwalek, and D. A. Sinclair, "Therapeutic Potential of NAD-Boosting Molecules: The *In vivo* Evidence," *Cell Metab.*, vol. 27, no. 3, pp. 529–547, Mar. 2018, doi: 10.1016/j.cmet.2018.02.011.
- [58] H. Bulluck and D. J. Hausenloy, "Modulating NAD⁺ metabolism to prevent acute kidney injury," *Nat. Med.*, vol. 24, no. 9, pp. 1306–1307, 2018, doi: 10.1038/s41591-018-0181-9.
- [59] A. Petrosyan *et al.*, "A glomerulus-on-a-chip to recapitulate the human glomerular filtration barrier," *Nat. Commun.*, vol. 10, no. 1, 2019, doi: 10.1038/s41467-019-11577-z.
- [60] F. Schutgens *et al.*, "Tubuloids derived from human adult kidney and urine for personalized disease modeling," *Nat. Biotechnol.*, vol. 37, no. 3, pp. 303–313, 2019, doi: 10.1038/s41587-019-0048-8.
- [61] K. I. W. Kane *et al.*, "Automated microfluidic cell culture of stem cell derived dopaminergic neurons," *Sci. Rep.*, vol. 9, no. 1, pp. 1–12, 2019, doi: 10.1038/s41598-018-34828-3.

Supplementary Data

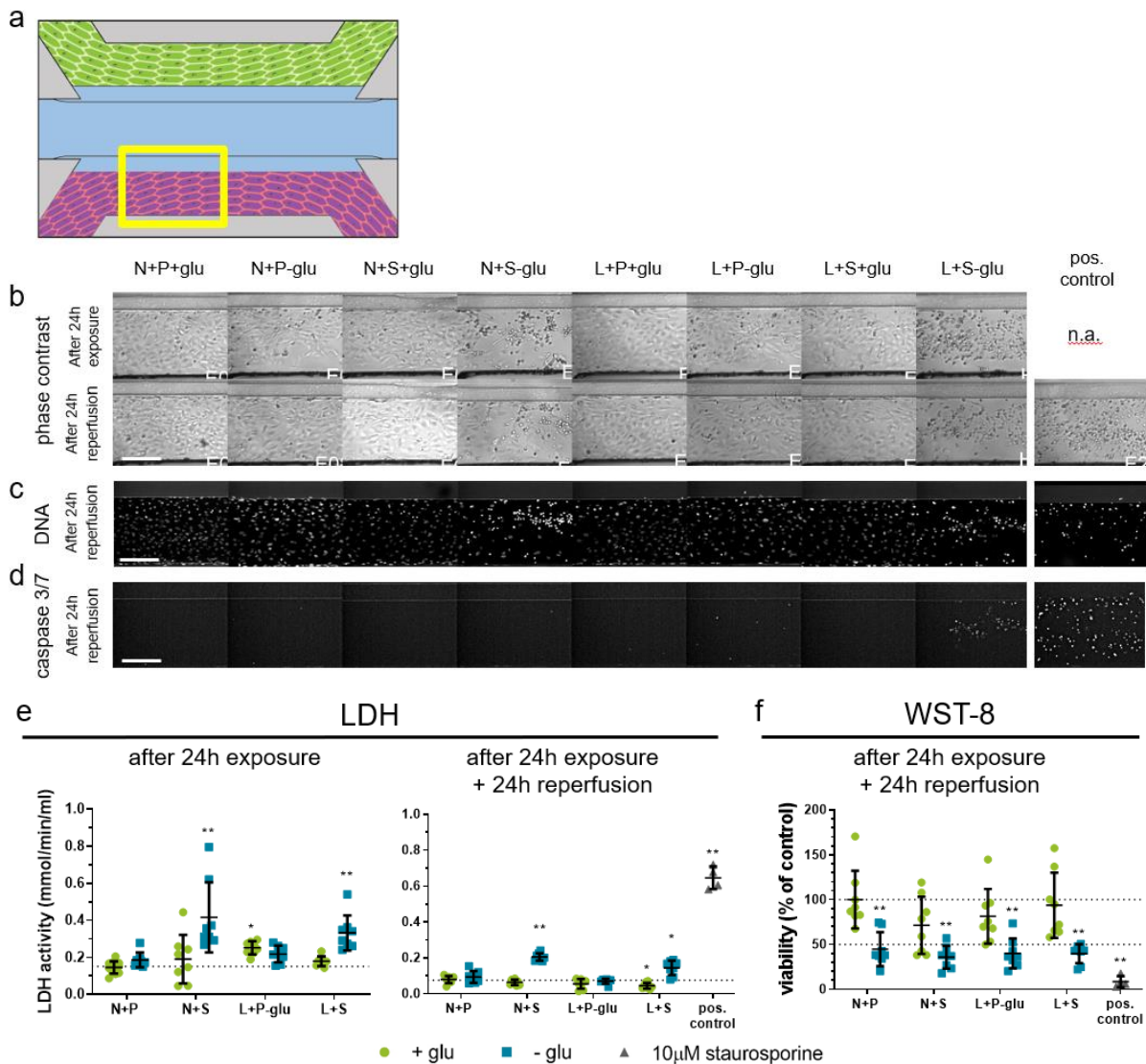


Figure S1: Modelling AKI upon ischemic parameter exposure showing results of HUVEC. Ischemia was modelled on the OrganoPlate by exposing the coculture to a combination of low oxygen (L), static incubation (S), and glucose and nutrient poor medium (-glu) for 24-hours, followed by a 24h reperfusion in normoxia (N), perfusion on the rocker (P), and in glucose and nutrient rich medium (+glu). **a** Region of the HUVEC vessel (yellow square) that is used for the images shown in b-d. **b** Representative phase-contrast images after 24-hour exposure (top) and subsequent 24-hour reperfusion (bottom). Different ischemia inducing conditions were tested (columns) and compared to the normal condition N+P+glu. N.a.= not available. **c** DNA staining after 24h reperfusion. **d** Caspase 3-7 staining after 24h reperfusion. Scalebar = 200µm. **e** LDH release in the medium was measured after 24h exposure (left) and 24h exposure plus 24h reperfusion (right) respectively. **f** WST-8 viability relative to the normal condition N+P+glu was assessed after 24h reperfusion. 10µM staurosporine was included as a positive control. Error bars represent standard deviation. One-way ANOVA compares the conditions to the N+P+glu control condition, ** $p < 0.01$ $n = 8-16$ chips per condition.

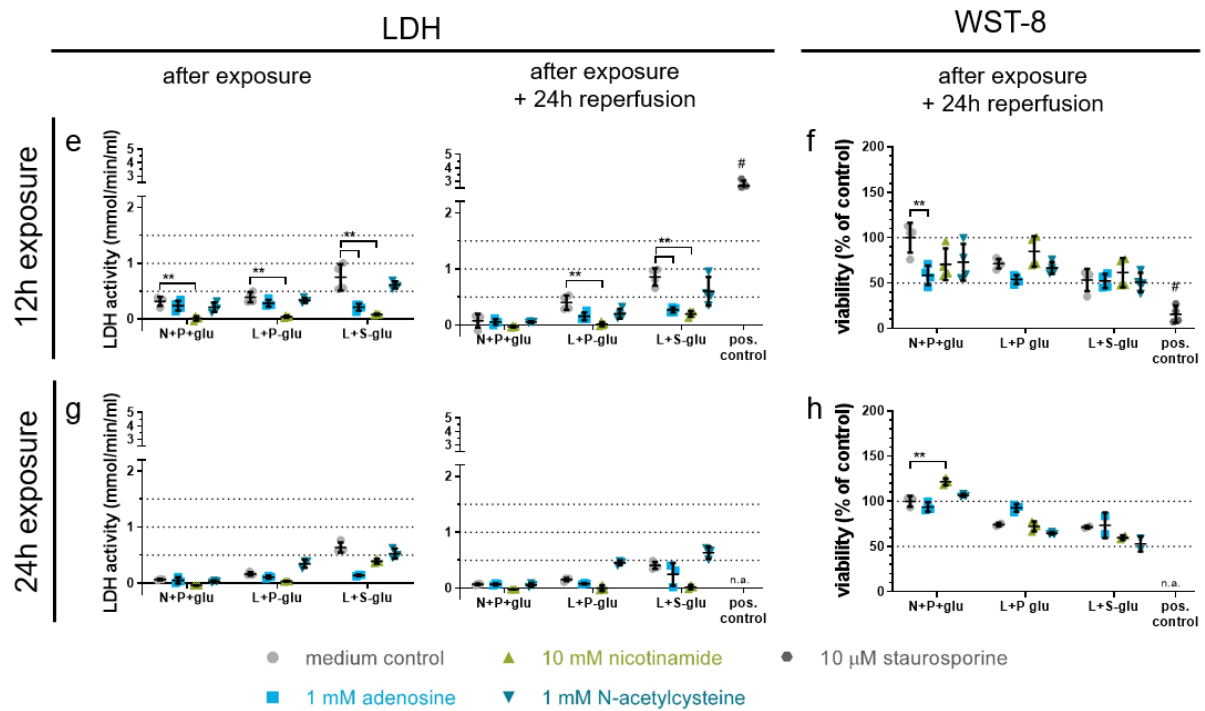
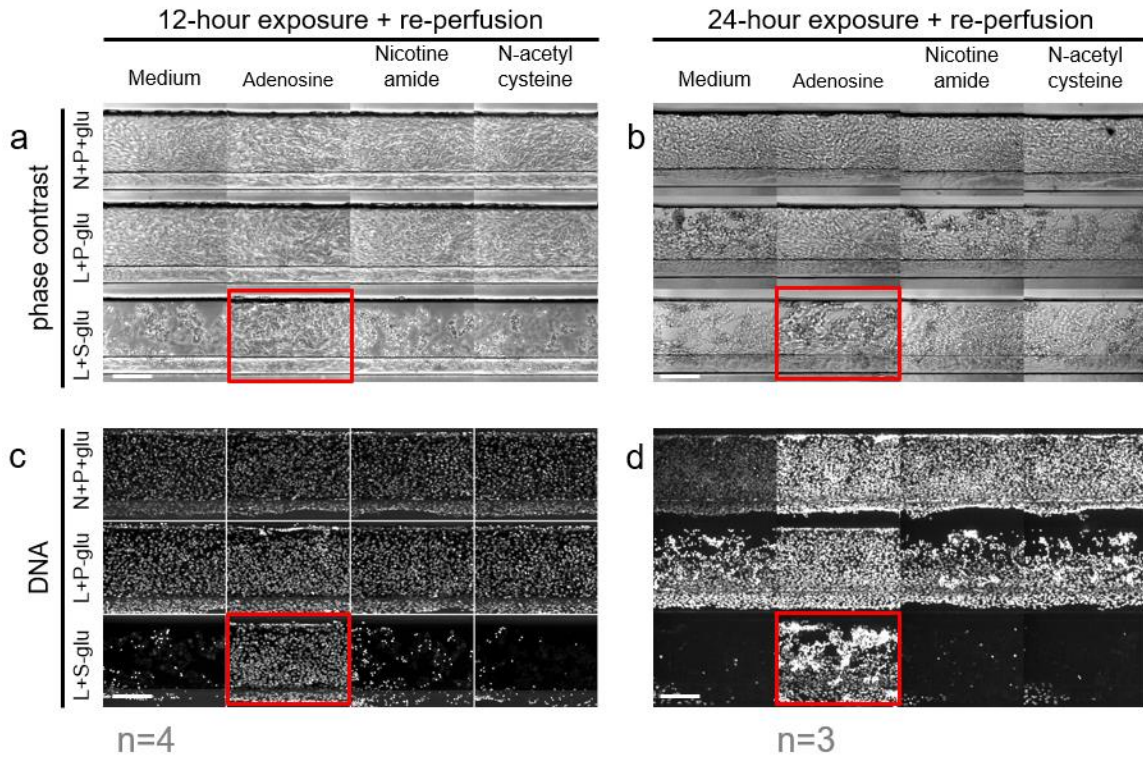


Figure S2: **Repetition of experimental data presented in figure 5 of the main text. Cultures were exposed to the selected ischemic conditions L+P-glu and L+S-glu for either 12 or 24 hours, followed by a 24 hour reperfusion, in the presence of adenosine, nicotinamide or N-acetylcysteine. N+P+glu medium only is the normoxic control condition. a-d** A zoom of the RPTEC tubule (see Fig. 4b) was imaged after 12-hour exposure and reperfusion (a, c) or after 24-hour exposure and reperfusion (b, d). Red squares indicate a protective effect of adenosine compared to the medium control of the same ischemic condition in phase contrast imaging and DNA staining. Scalebar = 200 μ m. **e-h** After the ischemic exposure of either 12 hours (e, f) or 24 hours (g, h) and a reperfusion of 24 hours for both, medium from the RPTEC channel was sampled and analyzed for LDH activity (e, g) and WST-8 viability relative to the N+P+glu medium control (f, h) was determined. One-way ANOVA compares the co-incubations to the medium control of the same ischemic condition, * $p < 0.05$, ** $p < 0.01$. # indicates the positive control differs significantly with all medium controls ($p < 0.01$). Error bars represent the standard deviation. 10 μ M staurosporine was included as a positive control. $n=3-4$ chips per condition.

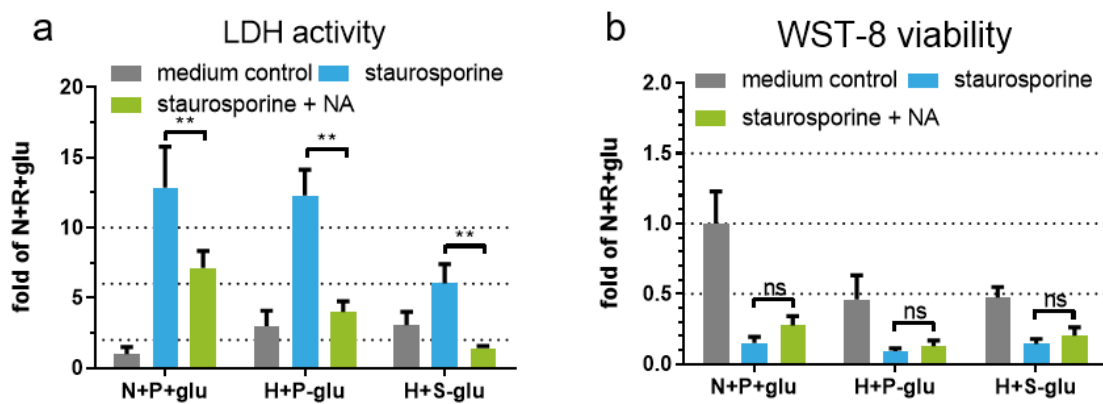


Figure S3: **LDH activity and WST-viability measured on cocultures exposed to staurosporine with and without co-incubation of nicotinamide (NA).** **a** LDH activity was significant lower when cocultures exposed to staurosporine were co-incubated with NA. **b** WST-8 viability was not significant higher when cocultures exposed to staurosporine were co-incubated with NA, indicating no protective effect of NA. ** $p < 0.01$. ns: not significant. Error bars represent the standard deviation. $n=4-8$ chips per condition.

Supplemental movie for figure 6 will be available online when published

